Tracks in Metals by MeV Fullerenes

H. Dammak, A. Dunlop, and D. Lesueur
Laboratoire des Solides Irradiés, Commissariat à l'Energie Atomique/Ecole Polytechnique, 91128 Palaiseau, France

A. Brunelle, S. Della-Negra, and Y. Le Beyec
Institut de Physique Nucléaire, CNRS-IN2P3, 91406 Orsay, France
(Received 22 July 1994)

It is shown that new specific effects take place during irradiation of metals with high energy fullerene beams. The observed quasicontinuous damage is confined inside ~20 nm diam cylinders around the projectile paths and is compared to the damage resulting from GeV heavy ion irradiation. The large extension of the highly damaged zones after cluster irradiations might be due to the strong localization of the deposited energy during the slowing-down process.

PACS numbers: 61.80.Lj, 61.80.Jh

It is now well accepted that electronic excitation and ionization arising from the slowing down of swift heavy ions can lead to structural modifications in bulk metallic targets as it has been known for a long time in insulators [1] and in thin [2] or discontinuous [3,4] metallic films. These modifications resulting from the high rates of energy deposition, which can reach values as high as 10 keV/nm, were unexpected in metallic materials where numerous and very mobile charge carriers allow a fast spreading of the deposited energy and an efficient screening of the space charge created in the projectile wake [5]. The main difference between insulators and conductors lies in the threshold above which the linear rate of energy deposition can lead to structural modifications.

So it has been shown that irradiation of bulk metallic targets with swift heavy ions can induce effects as varied as the so-called growth phenomenon of amorphous alloys [6,7], the amorphization of metal-metalloid alloys [8] or metal-metal alloys [9], a phase transformation in pure titanium [10], and defect creation in pure iron and zirconium [11]. The question of the transformation of the energy deposited by the projectile during the slowing-down process into energy stored in the target as lattice defects is still to be answered. Two mechanisms have been proposed: (i) The thermal spike model [12] in which the kinetic energy of the ejected electrons is transmitted to the lattice by electron-phonon interaction in a way efficient enough to increase the local lattice temperature above the melting point. This temperature increase is then followed by a rapid quenching. (ii) The Coulomb explosion model [13] in which the electrostatic energy of the space charge created just after the ion passage is converted into coherent radial atomic movements leading to a cylindrical shock wave.

Both mechanisms are sensitive to the rate of energy loss (dE/dx) as well as to the deposited energy density. The volume in which the energy is deposited scales with the range of the δ electrons—emitted during the ionization process—which depends only on the projectile velocity v. In monatomic ion irradiation it is not possible to vary significantly one of these parameters, say, v, keeping the second one unchanged, say, dE/dx, whereas it is easier using cluster ions. The aim of this paper is to compare damage induced in metallic targets (Ti, Zr) by MeV cluster ions with that previously observed [10,11] after irradiation with GeV heavy ions. The linear energy loss of MeV clusters (evaluated below) is comparable to that of GeV heavy ions, whereas their velocity is 1 order of magnitude lower (see Table I).

TABLE I. Characteristics of the experiments presented in this Letter. E_m is the maximum energy of the δ electrons (see text).

Target	Projectile	Incident energy (MeV)	$(dE/dx)_n$ (keV/nm)	$(dE/dx)_e$ (keV/nm)	E_m (eV)	Observations
Ti	Pb	845	0.08	36	8800	Dotted tracks Diameter ~5 nm
	C_{60}	18	1.8	43	50	Quasicontinuous tracks Diameter ~15 to 25 nm
Zr	U	5550	0.03	41	49 000	No observable damage
	C_{60}	18	1.8	44	50	Dotted tracks Diameter ~10 to 20 nm

This study has been made possible because of the energetic clusters that are now available at the tandem accelerator at the IPN Orsay where, for example, charged fullerene ions with energies ranging from 8 to 30 MeV have been accelerated [14]. Negative molecular C_{60}^- ions are accelerated in the first section of the tandem accelerator. At the positive high voltage terminal in the center of the accelerator (4 to 15 MV), the negative C_{60}^- ions collide with N_2 molecules in a stripper cell and become positively charged. Multiply charged C_{60}^{n+} (with $n \leq 4$) are formed, and it has been argued theoretically [15] that multiple ionization can occur only in plural binary collisions with nitrogen atoms passing through the fullerene. Time-of-flight (TOF) measurements combined with a magnetic deflection at a small angle (1.5°) allow us to identify unambiguously the beam of C_{60}^{1+} that has been used in this experiment. Figure 1 presents a TOF spectrum of C_{60}^{1+} measured at this deflecting angle of 1.5°. The beam intensity on the target varies between 10^5 and 10^6 projectiles per second on an area of 10 mm^2.

Pure titanium and zirconium targets [16], suitable for transmission electron microscopy observations (i.e., thickness ~100 nm), have been irradiated at 300 K with C_{60} under normal incidence up to a fluence of 10^{10} cm^{-2}. Figure 2 shows the corresponding electron micrographs of titanium irradiated by 18 MeV C_{60} molecules and, for comparison, electron micrographs of titanium irradiated by 845 MeV Pb ions. It must be noticed that in this case (GeV ion irradiations) the experimental procedure was slightly different [10]. The samples (~15 μm thick) are electrochemically thinned after irradiation in order to observe slices located at about 7 μm from the surfaces. This procedure ensures that the energy deposited in the observed part of the sample corresponds totally to the energy loss of the projectile. In both cases, observations under normal and tilted incidences are presented in order to illustrate that the damage takes place in a cylindrical region around the projectile path. After irradiation with monatomic Pb beams, the contrast in the microscope consists of small dots of average diameter 5 nm, the characteristic distance between these dots being close to 30 nm. The analysis of the images shows that the contrast is associated to dislocation loops located in the prismatic planes of the hexagonal structure [17]. After irradiation with C_{60} beams, the observed damaged zones entirely go through the sample thickness with an almost constant diameter of 20 nm. The analysis of the images shows that the contrast cannot be associated to microcrystallized matter nor to amorphous phase, but corresponds to a dense dislocation loop network. The detailed study of these contrasts is not yet completed and will be published elsewhere.

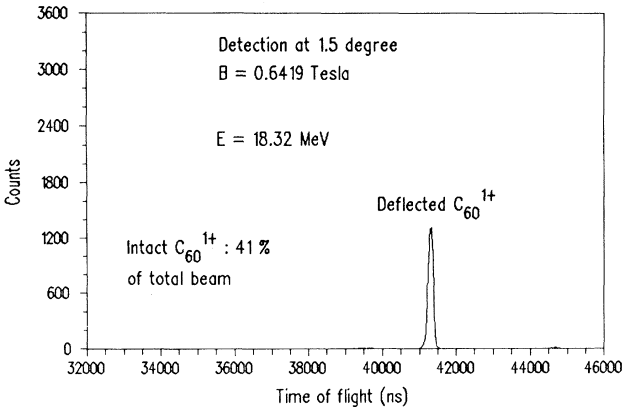

Fig. 1. Time-of-flight spectrum of a high energy fullerene beam obtained after magnetic deflection at 1.5°. The terminal voltage of the tandem accelerator is 9 MV and the C_{60}^- ion beam is pulsed before the entrance of the accelerator. There are intact only C_{60}^+ at 18.32 MeV at the target site.

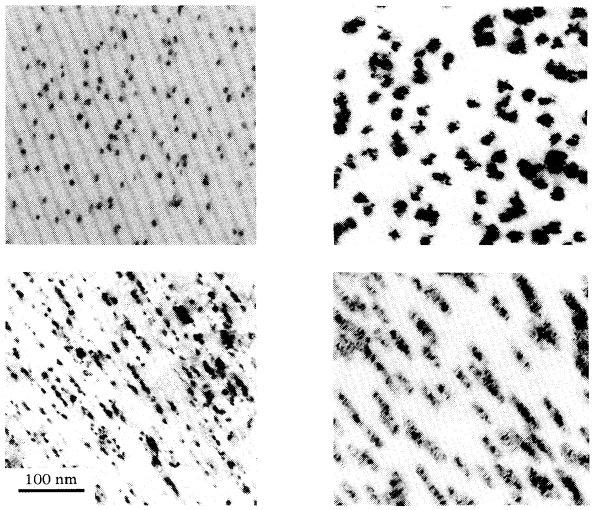

Fig. 2. Bright field images of titanium irradiated at 300 K: (a) with 845 MeV lead ions up to a fluence of 10^{11} cm^{-2} and (b) with 18 MeV C_{60} up to a fluence of 6×10^{10} cm^{-2}. In the upper part the electron beam direction is parallel to the ion beam. (a) Kinematic condition. (b) Two beam condition with $\mathbf{g} = \{101\}$. In the lower part, the sample is tilted in the microscope. (a) Tilt angle 26°; two beam condition with $\mathbf{g} = \{101\}$) and (b) tilt angle 30°; kinematic condition with $\mathbf{k}_0 \parallel [354]$).

It is worth noticing that there is a one to one correspondence between the numbers of impinging projectiles and observed "tracks." The radial extension and the longitudinal distribution of the damage demonstrate the very large efficiency of the C_{60} beam to create tracks.

Figure 3 shows electron micrographs of zirconium irradiated by 18 MeV C_{60} molecules. In this case micrographs corresponding to samples irradiated by swift heavy ions (prepared as mentioned above for titanium targets [10]) are not presented because they do not exhibit any contrast ascribable to damaged zones greater than the electron microscope resolution. This enforces the greater

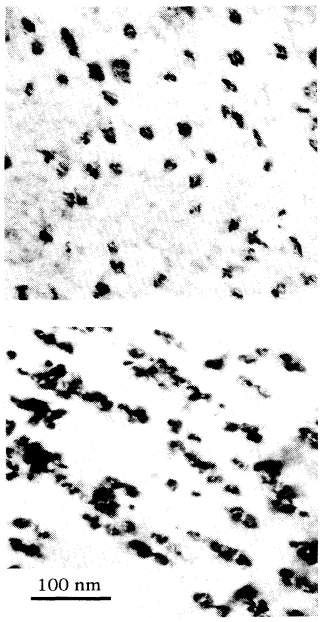

Fig. 3. Two beam condition bright field images of zirconium irradiated at 300 K with 18 MeV C_{60} molecules up to a fluence of 3.1×10^{10} cm^{-2}. In the upper part the electron beam direction is parallel to the ion beam ($\mathbf{g} = \{101\}$), whereas in the lower one, the sample is tilted by 36° in the microscope ($\mathbf{g} = \{100\}$).

efficiency of aggregate beams in producing damage in metallic targets.

The determination of the rate of energy deposition for clusters is still, to our knowledge, an open question from experimental and theoretical points of view. It is admitted that an aggregate entering a solid breaks into several fragments. However, the cylindrical shape of the damaged regions shows that these different fragments keep a close spatial correlation during the slowing-down process at least up to the sample thickness (100 to 200 nm). In order to estimate the energy deposited in both electronic excitation and nuclear collisions, it has been assumed that the energy loss of the initial C_{60} molecule is the sum of the energy losses of 60 individual carbon atoms.

As far as elastic collisions are concerned, the rate of energy deposition $(dE/dx)_n$ (see Table I) and the number of displaced atoms have been evaluated. Each C_{60} molecule would lead in such an approach to eight displacements every interatomic distance [19]. This number is certainly much too low to account for the huge observed damaged zones. Moreover, a complementary irradiation of a thin titanium foil was performed on the ARAMIS facility [20] at Orsay with 2.4 MeV Au_3 clusters. In this experiment, although each cluster induces about 30 atomic displacements every interatomic distance, no damage has ever been observed in the electron microscope after irradiations at fluences of 2×10^{10} or even 9×10^{12} clusters/cm^2. So, as in the case of GeV heavy ions [11], the damage induced by MeV C_{60} projectiles cannot result from the sole elastic collisions.

As far as inelastic collisions are concerned, the use of the above sum rule to calculate the rate of energy deposition $(dE/dx)_e$ (reported in Table I) implies that the equilibrium charge state reached by each individual carbon atom is not affected by the close vicinity of the other fragments. This hypothesis is based on the following remark: The main contribution to the slowing down comes from close collisions in which the impact parameter is smaller than the interatomic distance in the C_{60} molecule. As a matter of fact, the sole experimental results available in this field concerns measurements of the energy loss of C_{60} projectiles in thin (30 to 50 nm thick) amorphous carbon foils [18]. They show that the energy loss *per carbon* is, within the experimental uncertainty (about 5%), that of an individual carbon projectile of the same velocity.

The resulting stopping powers calculated with these assumptions are reported in Table I. As $(dE/dx)_e$ is always much larger than $(dE/dx)_n$, the range of the projectiles is governed by electronic energy losses. The ranges of 18 MeV C_{60} molecules (~490 nm in Ti and ~420 nm in Zr) are thus given by that of monatomic carbon of the same velocity. The thicknesses of the targets are much smaller than this range, so that the stopping region is avoided and that the electronic stopping power is almost constant throughout the sample thickness.

It appears that, although the rates of energy deposition in electronic excitation are close using monatomic GeV and aggregate MeV projectiles, both the radial and longitudinal characteristics of the damage differ strongly: Going from monatomic to aggregate beams, the radial extension increases markedly, whereas the longitudinal distribution evolves from a clearly dotted structure to a quasicontinuous one. The explanation for such different behaviors might originate from the great difference in the velocities of swift heavy ions and C_{60} projectiles. The transport of energy away is governed by δ electrons, which have an angular and a kinetic energy distribution related to the projectile velocity. Maximum kinetic energy values of δ electrons $E_m = 2mv^2$ (ejected in the forward direction) are given in Table I. For similar rates of energy deposition in electronic excitation, as the volume in which the energy is deposited is related to the radial range of secondary electrons, the lower the projectile velocity, the higher the energy deposition and, space charge densities. Using GeV Pb or U ions the radial range of the δ electrons is of some 1000 nm, whereas using a C_{60} beam, this radial range falls to a few interatomic distances. In this latter case, a crude estimate of the density of deposited energy by C_{60} ions leads to huge values as high as 10 eV/Å^3 (or 100 eV/atom). The relaxation of such a high energy density induces the spectacular struc-

tural modifications observed in this work. The damage is located inside a cylinder which has a radius at least 1 order of magnitude greater than the radius of the cylinder in which the primary energy is deposited.

Other new effects are expected to result from irradiation of solids with large MeV clusters as, for example, intense secondary emission.

[1] R. L. Fleischer, P. B. Price, and R. M. Walker, J. Appl. Phys. **36**, 3645 (1965).
[2] T. S. Noggle and J. O. Stiegler, J. Appl. Phys. **33**, 1726 (1962).
[3] K. L. Merkle, Phys. Rev. Lett. **9**, 150 (1962).
[4] H. H. Andersen, H. Knudsen, and P. Moller Petersen, J. Appl. Phys. **49**, 5638 (1978).
[5] This obviously does not apply to very thin metallic films or small size metallic clusters in which the spreading of the deposited energy is strongly limited by the close vicinity of the boundaries.
[6] S. Klaumünzer and G. Schumacher, Phys. Rev. Lett. **51**, 1987 (1983).
[7] A. Audouard, E. Balanzat, G. Fuchs, J. C. Jousset, D. Lesueur, and L. Thomé, Europhys. Lett. **3**, 327 (1987).
[8] A. Audouard, E. Balanzat, J. C. Jousset, A. Chamberod, A. Dunlop, D. Lesueur, G. Fuchs, R. Spohr, J. Vetter, and L. Thomé, Phys. Rev. Lett. **65**, 875 (1990).
[9] A. Barbu, A. Dunlop, D. Lesueur, and R. S. Averback, Europhys. Lett. **15**, 37 (1991).
[10] H. Dammak, A. Barbu, A. Dunlop, D. Lesueur, and N. Lorenzelli, Philos. Mag. Lett. **67**, 253 (1993).
[11] A. Dunlop and D. Lesueur, Radiat. Eff. Defects Solids **126**, 123 (1993).
[12] M. Toulemonde, C. Dufour, and E. Paumier, Phys. Rev. B **46**, 14 362 (1992).
[13] D. Lesueur and A. Dunlop, Radiat. Eff. Defects Solids **126**, 163 (1993).
[14] S. Della-Negra, A. Brunelle, Y. Le Beyec, J. M. Curaudeau, J. P. Mouffron, B. Waast, P. Hakansson, B. U. R. Sundquist, and E. S. Parilis, Nucl. Instrum. Methods Phys. Res., Sect. B **74**, 453 (1993).
[15] E. S. Parilis, Nucl. Instrum. Methods Phys. Res., Sect. B **88**, 21 (1994).
[16] The dominant impurity is oxygen with an atomic concentration lower than 100 ppm.
[17] J. Henry, A. Barbu, B. Leridon, D. Lesueur, and A. Dunlop, Nucl. Instrum. Methods Phys. Res., Sect. B **67**, 390 (1992).
[18] K. Baudin, A. Brunelle, M. Chabot, S. Della-Negra, J. Depauw, D. Gardes, P. Hakansson, Y. Le Beyec, A. Billebaud, M. Fallavier, J. Remilleux, J. C. Poizat, and J. P. Thomas, Nucl. Instrum. Methods Phys. Res., Sect. B **94**, 341 (1994).
[19] J. P. Biersack, in *Ion Beam Modifications of Insulators,* edited by P. Mazzoldi and G. W. Arnold (Elsevier, Amsterdam, 1987), p. 1.
[20] The authors wish to acknowledge the useful help of the ARAMIS facility team, especially Dr. J. Chaumont, for the gold cluster irradiations.

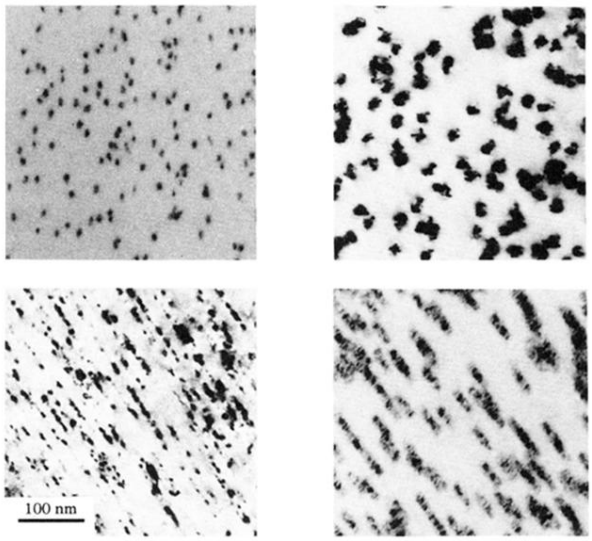

Fig. 2. Bright field images of titanium irradiated at 300 K: (a) with 845 MeV lead ions up to a fluence of 10^{11} cm^{-2} and (b) with 18 MeV C_{60} up to a fluence of 6×10^{10} cm^{-2}. In the upper part the electron beam direction is parallel to the ion beam. (a) Kinematic condition. (b) Two beam condition with $\mathbf{g} = \{101\}$. In the lower part, the sample is tilted in the microscope. (a) Tilt angle 26°; two beam condition with $\mathbf{g} = \{101\}$) and (b) tilt angle 30°; kinematic condition with $\mathbf{k}_0 \parallel [354]$).

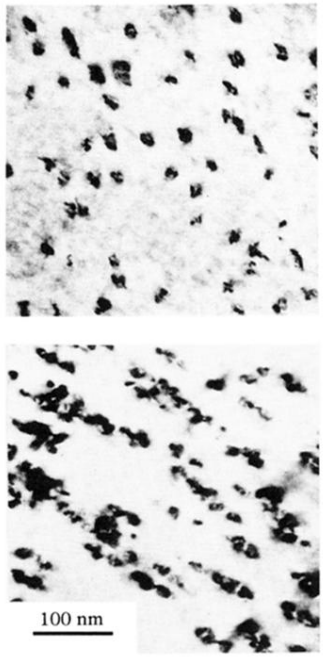

Fig. 3. Two beam condition bright field images of zirconium irradiated at 300 K with 18 MeV C_{60} molecules up to a fluence of 3.1×10^{10} cm^{-2}. In the upper part the electron beam direction is parallel to the ion beam ($\mathbf{g} = \{101\}$), whereas in the lower one, the sample is tilted by 36° in the microscope ($\mathbf{g} = \{100\}$).